

Determining Neutrino Mass from the CMB Alone

Manoj Kaplinghat, Lloyd Knox and Yong-Seon Song
 Department of Physics, One Shields Avenue
 University of California, Davis, California 95616, USA
 (Dated: October 21, 2019)

Distortions of Cosmic Microwave Background (CMB) temperature and polarization maps caused by gravitational lensing, observable with high angular resolution and high sensitivity, can be used to measure the neutrino mass. We show how the lensing signature in the CMB breaks a degeneracy between neutrino mass, dark energy equation of state and the primordial power spectrum amplitude, allowing for their simultaneous determination. Assuming two massless species and one with mass m we forecast $(m) = 0.14$ eV from the Planck satellite and $(m) = 0.03$ eV from observations with twice the angular resolution and 20 times the sensitivity. A detection is likely at this higher sensitivity since the observation of atmospheric neutrino oscillations require $m^2 > (0.04\text{eV})^2$.

Introduction. Results from the WMAP [1] show the standard cosmological model passing a highly stringent test. With this spectacular success of the CMB as a clean and powerful cosmological probe, and of the standard model as a phenomenological description of nature, it is timely to ask what can be done with yet higher resolution and higher sensitivity such as offered by the Planck instruments and beyond. In this Letter we mostly focus on neutrino mass determination, with brief discussion of other applications.

Eisenstein et al. [2] found that the Planck satellite can measure neutrino mass with an error of 0.26 eV. This sensitivity limit is related to the temperature at which the plasma recombines and the photons last scatter off the free electrons, $T_{\text{dec}} \approx 0.3$ eV. Neutrinos with $m < T_{\text{dec}}$ do not leave any imprint on the last-scattering surface that would distinguish them from $m = 0$.

Neutrinos with mass $m < T_{\text{dec}}$ would affect the amplitudes of gravitational potential peaks and valleys at intermediate redshifts. Massive neutrinos can collapse into potential wells when they become non-relativistic, while massless ones freely stream out. The observed galaxy power spectrum (which is proportional to the potential power spectrum at sufficiently large scales), combined with CMB observations can be used to put constraints on m [3]. At present such an analysis yields an upper bound on m of 0.3 eV [4][46].

The alteration of the gravitational potentials at late times changes the gravitational lensing of CMB photons as they traverse these potentials [5, 6]. Including the gravitational lensing effect, we find that the Planck error forecast improves to 0.14 eV. We also show that more ambitious CMB experiments can reduce this error to 0.03 eV. These mass ranges are interesting because the atmospheric neutrino oscillations require that at least one of the active neutrinos have $m > 0.04$ to 0.1 eV.

Topographic observations of the galaxy shear due to gravitational lensing can achieve sensitivities to m similar to what we find here assuming the lensed galaxies can be cleanly separated into $z = 0.1$ redshift slices over 10% of the sky [7, 8]. Our work here is distinguished by

its sole reliance on CMB temperature and polarization maps which have different potential sources of systematic error. Complementary techniques are valuable since both of these will be very challenging measurements.

The most stringent laboratory upper bound on neutrino mass comes from tritium beta decay end-point experiments [9] which limit the electron neutrino mass to < 2 eV. Proposed experiments plan to reduce this limit by one to two orders of magnitude by searching for neutrinoless double beta decay ($\beta\beta 0\nu$) [10]. A Dirac mass would elude this search, but theoretical prejudice favors (and the see-saw mechanism requires) Majorana masses. Like the CMB and galaxy shear observations, these future $\beta\beta 0\nu$ experiments will be extremely challenging. Lensing of the CMB. The intensity and linear polarization of the CMB are completely specified by the Stokes parameters, I, Q and U which are related to the unlensed Stokes parameters (denoted with a tilde) by $X(\tilde{n}) = X(\tilde{n} + \tilde{n})$ where X stands for I, Q or U . The deflection angle, n , is the tangential gradient of the projected gravitational potential,

$$n = 2 \frac{dr}{r} \frac{(r - r_s)}{rr_s} \quad (\tilde{n}; r); \quad (1)$$

where r is the coordinate distance along our past light cone, s denotes the CMB last-scattering surface, \tilde{n} is the unit vector in the n direction and \tilde{n} is the three-dimensional gravitational potential.

The statistical properties of the I, Q and U maps are most simply described in the transform space: $a_T(l)$, $a_E(l)$, and $a_B(l)$ where a_T is the spherical harmonic transform of I and a_E and a_B are the curl-free and gradient-free decompositions, respectively, of Q and U [11, 12]. In this transform space the effect of lensing by mode (L) is to shift power from, e.g., $a_T(L-1)$ to $a_T(L)$. Lensing also mixes a_E into a_B and any a_B into a_E [13].

This mixing of modes leads to three qualitatively different effects in the statistical properties of a_T , a_E and a_B . The first is a smearing out of the features in the two-point functions, also called angular power spectra, C_l , where $\langle a_T(l) a_T(l') \rangle = C_l \delta(l-l') = 2 \int l(l+1)$ and

stands for either T, E, or B [5]. See Fig. 1. Through lensing, peaks smooth down, and the exponential drop in power at high l due to the thickness of the last scattering surface becomes a power law. The second effect is the generation of B modes (see Fig. 2).

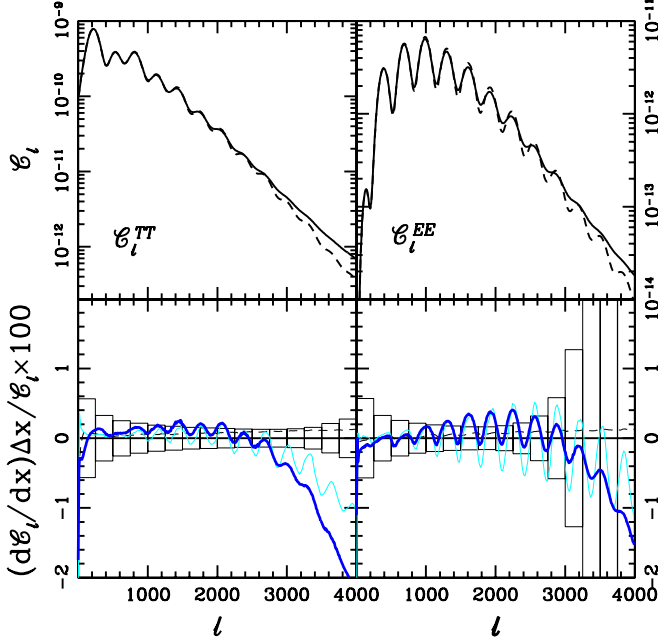


FIG. 1: Top panels: angular power spectra C_1^{TT} (left) and C_1^{EE} (right) for the ducial model ($m = 0$) with no lensing (dashed) and with lensing (solid). Bottom panels: $100 \frac{dC_1^{TT}}{dm} = dm$ ($m = C_1^{TT}$) (dark) and $100 \frac{dC_1^{TT}}{dw_x} (w_x = C_1^{TT})$ (light) for $m = 0.3$ eV and $w_x = 0.2$. Same for C_1^{EE} .

The third effect is in the four-point functions, e.g., $\hat{a}_T(l_1)a_T(l_2)a_E(l_3)a_B(l_4)i$ [6, 14, 15, 16]. Here we do not directly consider any four-point functions but rather the two-point function of the lensing potential, C_1 , which can be inferred from the map 4-point functions [17]. In Fig. 2 we plot the deflection angle power spectrum, C_1^{dd} , $l(l+1)C_1$.

We use a publicly available numerical solver of the Boltzmann and Einstein equations, CMBfast [5], to calculate the four non-zero map two-point functions: C_1^{TT} , C_1^{EE} , C_1^{TE} and C_1^{BB} . We modified CMBfast to include a scalar field component that acts as dark energy, to include the effect of massive neutrinos on the recombination history (through the expansion rate), to calculate lensing at high m more accurately and to calculate C_1 . We neglect C_1^T which may be useful for studying model-dependent clustering properties of the dark energy [18]. We use the Peacock and Dodds prescription to calculate the non-linear matter power spectrum [19]. More details are in [20].

Effect of neutrinos. The lower panels in Figures 1 and 2 show the differences in the power spectra between our

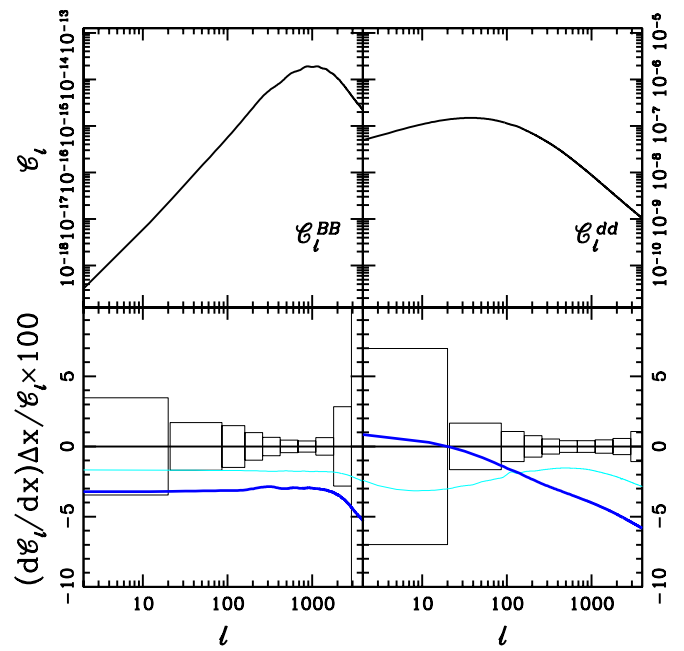


FIG. 2: Top panels: angular power spectra C_1^{BB} with no tensor contribution (left) and C_1^{dd} (right) for the ducial model ($m = 0$). Bottom panels: same as for Fig. 1 but for C_1^{BB} and C_1^{dd} .

ducial model and the exact same model but with one of the three neutrino masses altered from zero to 0.1 eV. The error boxes are those for CMBpol (described below; see Table 1). For C_1^{TT} , the errors at $l < 2000$ are entirely due to sample variance; the accuracy is limited by the finite number of modes at each l value on the sky, and not by instrumental noise. For the much weaker C_1^{BB} signal instrumental noise is the dominant source of error at all l values.

The signature of a 0.1 eV neutrino in the angular power spectra, in the absence of lensing, is at the 0.1% level as shown in Fig. 1. Such small masses are only detectable through their effect on lensing, which comes through their influence on the gravitational potential. Replacing a massless component with a massive one increases the energy density and therefore the expansion rate, suppressing growth. The net suppression of the power spectrum is scale dependent and the relevant length scale is the Jeans length for neutrinos [21, 22, 23] which decreases with time as the neutrino thermal velocity decreases. This suppression of growth is ameliorated at scales larger than the Jeans length at matter-radiation equality where the neutrinos can cluster because of their non-zero mass. Neutrinos never cluster at scales smaller than the Jeans length today. The net result is no effect on large scales and a suppression of power on small scales, resulting in the shape of $C_1^{dd} = C_1^{BB}$ in Figure 2.

The wiggles in the differences $\hat{C}_1^T = C_1^{TT}$ and $\hat{C}_1^E = C_1^{EE}$ are due to differences in lensing. Lensing sup-

presses peaks, boosts troughs and has little effect on injection points. Thus the result of decreasing the lensing power is an oscillatory pattern in the change in the lensing correction, with the same frequency and phase as the peak structure of the fiducial model. The effect is more pronounced at higher l where the lensing correction is larger and consistently positive.

Error forecasting method. The distortions to the angular power spectra due to a 0.1 eV neutrino are very small. We have taken care to accurately forecast the constraints possible in this mass range. To calculate the expected errors on m , and all the other cosmological parameters we must simultaneously solve for, we make a first order Taylor expansion of the parameter dependence of all the two-point functions. In this ‘linear response’ approximation, given the expected experimental errors on the power spectra, we can easily calculate the expected parameter error covariance matrix.

The linear response approximation is improved and susceptibility to numerical error is reduced with a careful choice of the parameters used to span a given model space [2, 24, 25, 26]. We take our set to be $P = f_{\text{m}}; f_{\text{b}}; f_{\text{s}}; w_x; z_{\text{reion}}; k^3 P^i(k_f); n_s; n_s^0; y_{\text{He}}g$. The first three of these are the densities today (in units of $1.88 \cdot 10^{-29} \text{ g/cm}^3$) of cold dark matter plus baryons, baryons and massive neutrinos. Next two are the angular size subtended by the sound horizon on the last-scattering surface and the ratio of dark energy pressure to density. Reionization of the intergalactic medium (IGM) is assumed to happen suddenly at z_{ri} and the primordial potential power spectrum is assumed to be $k^3 P^i(k) = k_f^3 P^i(k_f) (k=k_f)^{n_s - 1 + n_s^0 \ln(k/k_f)}$ with $k_f = 0.05 \text{ Mpc}^{-1}$. The fraction of baryonic mass in Helium (which affects the number density of electrons) is y_{He} . We Taylor expand about $P = f_0: 1.46; 0.021; 0.06; 1.63; 6.4 \cdot 10^{-11}; 1; 0; 0.24g$. The Hubble constant for this model is $h = 0.655$ where $H_0 = 100h \text{ km sec}^{-1} \text{ Mpc}^{-1}$.

We follow [27] to calculate the errors expected in C_1^{TT} , C_1^{TE} , C_1^{EE} and C_1^{BB} given Table 1, assuming the maps are Gaussian random fields. The non-Gaussianity caused by lensing increases the noise and correlates errors between different l values. The net degradation in total signal-to-noise is less than about 5% for the experiments we consider [28]. For errors on C_1 we follow [17]. Correlations in the errors between C_1 and the other power spectra are small [20].

Experiments. We consider Planck [29], a high-resolution version of CMBpol [47], and a polarized bolometer array on the South Pole Telescope [48] we will call SPTpol. Their specifications are given in Table 1. We assume that other frequency channels of Planck and CMBpol (not shown in the table) will clean out non-CMB sources of radiation perfectly. Detailed studies have shown foreground degradation of the results expected from Planck

Experiment	$\ell_{\text{max}}^{\text{T}}$	$\ell_{\text{max}}^{\text{EE}}$	(GHz)	b	T	P
Planck	2000	3000	100	9.2'	5.5	1
			143	7.1'	6	11
			217	5.0'	13	27
SPTpol ($f_{\text{sky}} = 0.1$)	2000	3000	217	0.9'	12	17
CMBpol	2000	3000	217	3.0'	1	1.4

TABLE I: Experimental specifications.

to be mild [30, 31, 32]. At $l > 3000$ emission from dusty galaxies will be a significant source of contamination. The effect is expected to be more severe for temperature maps. Hence we restrict temperature data to $l < 2000$ and polarization data to $l < 3000$. The results change very little if the polarization data is also restricted to $l < 2000$.

Results. We emphasize the ability of the experiments to simultaneously determine P^i , w_x and m [49]. These all affect the amplitude of P^i at late times, the latter two due to their effect on the rate of growth of density perturbations. If we were only sensitive to the amplitude of C_1 then there would be an exact degeneracy between these three parameters. However, the l -dependence of the response of C_1 to these parameter variations breaks this would-be degeneracy, allowing for their simultaneous determination.

There is a well-known way to determine P^i without use of the significantly-lensed angular scales: that is to combine C_1^{EE} and C_1^{TE} at $l < 20$ where they are proportional to $P^i e^2$ and P^i respectively [27, 33] with the TT, EE and ET spectra at $20 < l < 2000$ where they are proportional to $P^i e^2$. With P^i determined in this manner we expect $(\ln P^i) = 2$ ().

The remaining degeneracy to break is between m and w_x . We have already discussed the l -dependence of $\partial \ln C_1 / \partial m$ shown in Fig. 1 as resulting from the scale- and time-dependence of $\partial \ln P / \partial m$. The l -dependence of $\partial \ln C_1 / \partial w_x$ has the opposite sense. Although the suppression of P^i for increasing w_x is nearly k -independent, the effect is larger at late times | hence the radial projection gives a larger effect at low l . The effects of m and w_x are sufficiently distinct to allow for their simultaneous determination. Note that the effect of w_x is more pronounced for larger values due to two reasons. One, dark energy starts to dominate earlier (which implies larger uniform suppression) and two, perturbations in dark energy on large scales are enhanced for large w_x .

The $m = w_x$ degeneracy breaking is important since it allows for, e.g., Planck to detect the acceleration of the Universe ($w_x < 1 = (3 - x)$) at the 2 level. Such a con-

TABLE II:

Error Forecasts

Experiment	m (eV)	w_x	$\ln P^i$	n_s	n_s^0	s (deg)		$\ln \delta_m$	$\ln \delta_b$	y_{He}
Planck	0.14	0.28	0.016	0.0074	0.0032	0.0022	0.0081	0.0073	0.0081	0.012
SPTpol	0.11	0.34	0.018	0.01	0.0057	0.0033	0.0086	0.011	0.011	0.016
SPTpol+ Planck	0.082	0.22	0.016	0.0057	0.0027	0.0018	0.008	0.0062	0.0062	0.0096
CM Bpol	0.031	0.088	0.011	0.0024	0.0014	0.00074	0.0057	0.0026	0.0028	0.0039

NOTES. | Standard deviations expected from Planck, SPTpol and CM Bpol.

rmation would be valuable given the deep theoretical implications of acceleration [34]. Hu [18] has previously noted this result obtained with the assumption $m = 0$.

If we assume a single-step transition for the ionization history Planck can achieve $(\delta) = 0.005$ [2]. However, foreground contamination [31], and modeling uncertainty in the ionization history [35] can increase this uncertainty. For these reasons we conservatively ignore polarization data at $l < 30$ and instead set a prior, by hand, of $(\delta) = 0.01$; including the $l < 30$ polarization data would (perhaps artificially) achieve a smaller (δ) .

We note that the non-linear dependence of the lensed spectra on P^i leads to it being better determined than twice the (δ) prior we impose (see Table 2). For CM Bpol, the forecasted error on P^i is about 1% and the resulting (δ) is 0.005.

An extended period of reionization, as suggested by the combination of WMAP and quasar observations [36], would probably have large spatial fluctuations in the ionization fraction. Such "patchy" reionization may lead to a large diffuse kinetic SZ contribution to \mathcal{F}_1^T at high l [16, 37, 38, 39], possibly larger than the lensing contribution. Fortunately the analogous effect in the polarization is much smaller [39, 40]. For a conservative upper bound on how patchy reionization could degrade (δ) , we restrict the temperature data to $l < 1000$ and find $(\delta) = 0.035$ eV for CM Bpol and 0.092 eV for SPTpol+ Planck.

The primary motivation for CM Bpol is the detection of the B mode due to gravity waves produced in inflation. The amplitude of this signal would directly tell us the energy density during inflation. Following the calculation in [41] (see also [42]) we find a 3 detection is possible for CM Bpol if the fourth root of the energy density during inflation is greater than $E_{\text{in}} = 2 \cdot 10^{15}$ GeV which is an order of magnitude smaller than the GUT scale. We note that $E_{\text{in}}^4 / 1 = 1$, approximately, for $0.05 < \eta < 0.2$ and we have assumed $\eta = 0.1$. This scaling with η suggests the largest angular scales, where the reionization feature in the B mode appears, are important and therefore a

full-sky experiment is necessary to achieve this sensitivity level.

The scalar spectrum determined from high-resolution CMB observations can also be a useful probe of inflation, as studied recently by [43]. If $n_s - 1 = 0.07$, the central value in fits to WMAP and other observations [4], then inflationary models generically predict $n_s^0 - (n_s - 1)^2 = 0.005$ which will be detectable at the 3 level by CMBpol.

Determining δ_b and y_{He} to high precision will facilitate precision consistency tests with Big Bang Nucleosynthesis (BBN) predictions. It will also be useful in constraining non-standard BBN. For example, determining δ_b and y_{He} to high precision allows strong constraints to be put on the number of relativistic species N (or equivalently the expansion rate) during BBN. If (y_{He}) is small, then $(N) = (y_{He}) = 0.013$, which for CMBpol works out to $(N) = 0.2$. Constraints on N have important repercussions for neutrino mixing in the early universe, and hence on neutrino mass models [44].

Conclusions. Gravitational lensing of the CMB is a promising probe of the growth of structure and the fundamental physics that affects it. High sensitivity, high resolution maps will allow us to measure the lensing signature well enough to simultaneously constrain m , w_x and P . A future all-sky polarized CMB mission aimed at detecting gravitational waves is likely to succeed in determining neutrino mass as well.

We thank M. Kamionkowski, J. Bock, S. Church, A. Lange, S. Meyer and M. White for useful conversations.

- [1] C. L. Bennett et al, (2003), astro-ph/0302207.
- [2] D. J. Eisenstein, W. Hu, and M. Tegmark, Astrophys. J. 518, 2 (1999).
- [3] W. Hu, D. J. Eisenstein, and M. Tegmark, Phys. Rev. Lett. 80, 5255 (1998).
- [4] D. N. Spergel et al, (2003), astro-ph/0302209.
- [5] U. Seljak and M. Zaldarriaga, Astrophys. J. 469, 437 (1996).

[6] F. Bernardeau, *Astron. & Astrophys.* 324, 15 (1997).

[7] W. Hu and C. R. Keeton, *Phys. Rev. D* 66, 63506 (2002).

[8] W. Hu, *Phys. Rev. D* 66, 83515 (2002).

[9] J. Bonn et al., *Nucl. Phys. Proc. Suppl.* 110, 395 (2002).

[10] Y. Zdesenko, *Rev. Mod. Phys.* 74, 663 (2003).

[11] M. Kamionkowski, A. Kosowsky, and A. Stebbins, *Phys. Rev. Lett.* 78, 2058 (1997).

[12] U. Seljak and M. Zaldarriaga, *Phys. Rev. Lett.* 78, 2054 (1997).

[13] M. Zaldarriaga, U. Seljak, and E. Bertschinger, *Astrophys. J.* 494, 491 (1998).

[14] M. Zaldarriaga, *Phys. Rev. D* 62, 63510 (2000).

[15] T. O'kamoto and W. Hu, *Phys. Rev. D* 66, 63008 (2002).

[16] A. Cooray and M. Kesden, *New Astronomy* 8, 231 (2003).

[17] W. Hu and T. O'kamoto, *Astrophys. J.* 574, 566 (2002).

[18] W. Hu, *Phys. Rev. D* 65, 23003 (2002).

[19] J. A. Peacock and S. J. D. odds, *Mon. Not. Roy. Astron. Soc.* 280, L19 (1996).

[20] M. Kaplinghat, L. Knox, and Y.-S. Song, in preparation.

[21] J. R. Bond and A. S. Szalay, *Astrophys. J.* 274, 443 (1983).

[22] C. Ma, *Astrophys. J.* 471, 13 (1996).

[23] W. Hu and D. J. Eisenstein, *Astrophys. J.* 498, 497 (1998).

[24] G. Efstathiou and J. R. Bond, *Mon. Not. Roy. Astron. Soc.* 304, 75 (1999).

[25] W. Hu, M. Fukugita, M. Zaldarriaga, and M. Tegmark, *Astrophys. J.* 549, 669 (2001).

[26] A. Kosowsky, M. Milosavljevic, and R. Jimenez, *Phys. Rev. D* 66, 63007 (2002).

[27] M. Zaldarriaga, D. N. Spergel, and U. Seljak, *Astrophys. J.* 488, 1+ (1997).

[28] W. Hu, *Phys. Rev. D* 64, 83005 (2001).

[29] J. A. Tauber, in *IAU Symposium (PUBLISHER, ADDRESS, 2001)*, pp. 493{+}.

[30] L. Knox, *Mon. Not. Roy. Astron. Soc.* 307, 977 (1999).

[31] M. Tegmark, D. J. Eisenstein, W. Hu, and A. de Oliveira-Costa, *Astrophys. J.* 530, 133 (2000).

[32] F. R. Bouchet and R. Gispert, *New Astronomy* 4, 443 (1999).

[33] M. Kaplinghat et al., *Astrophys. J.* 583, 24 (2003).

[34] N. Kaloper et al., *JHEP* 11, 037 (2002).

[35] G. Holder, Z. Haiman, M. Kaplinghat, and L. Knox, (2003), [astro-ph/0302404](http://arxiv.org/abs/astro-ph/0302404).

[36] A. Kogut et al., (2003), [astro-ph/0302213](http://arxiv.org/abs/astro-ph/0302213).

[37] N. Aghanim, F. X. de Sa, J. L. Puget, and R. Gispert, *Astron. & Astrophys.* 311, 1 (1996).

[38] A. Gruzinov and W. Hu, *Astrophys. J.* 508, 435 (1998).

[39] L. Knox, R. Scoccimarro, and S. Dodelson, *Phys. Rev. Lett.* 81, 2004 (1998).

[40] J. Waller, *Astrophys. J. Lett.* 527, L1 (1999).

[41] L. Knox and Y.-S. Song, *Phys. Rev. Lett.* 89, 011303 (2002).

[42] M. Kesden, A. Cooray, and M. Kamionkowski, *Phys. Rev. Lett.* 89, 11304 (2002).

[43] B. Gold and A. A. Ibrecht, (2003), [astro-ph/0301050](http://arxiv.org/abs/astro-ph/0301050).

[44] K. N. Abazajian, (2002), [astro-ph/0205238](http://arxiv.org/abs/astro-ph/0205238).

[45] R. B. M. Etcalf and J. Silk, *Astrophys. J. Lett.* 492, L1 (1998).

[46] Published forecasts for combining Planck and the SDSS galaxy power spectrum [2, 23] show no significant improvement is expected.

[47] CMBpol: <http://space-science.nasa.gov/missions/concepts.htm>.

[48] SPT: <http://astro.uchicago.edu/spt/>

[49] The degeneracy-breaking power of CMB lensing was first pointed out for $\Omega = k$ in [45].